The scattered disk population as a source of Oort cloud comets: evaluation of its current and past role in populating the Oort cloud

Julio A. Fernández [a,*], Tabaré Gallardo [a], Adrián Brunini [b,c]

[a] *Departamento de Astronomía, Facultad de Ciencias, Iguá 4225, 11400 Montevideo, Uruguay*
[b] *Facultad de Ciencias Astronómicas y Geofísicas, Universidad Nacional de La Plata, Paseo del Bosque, 1900 La Plata, Argentina*
[c] *Instituto Astrofísico de La Plata, CONICET, Argentina*

Abstract

We have integrated the orbits of the 76 scattered disk objects (SDOs), discovered through the end of 2002, plus 399 clones for 5 Gyr to study their dynamical evolution and the probability of falling in one of the following end states: reaching Jupiter's influence zone, hyperbolic ejection, or transfer to the Oort cloud. We find that nearly 50% of the SDOs are transferred to the Oort cloud (i.e., they reach heliocentric distances greater than 20,000 AU in a barycentric elliptical orbit), from which about 60% have their perihelia beyond Neptune's orbit ($31 \text{ AU} < q < 36 \text{ AU}$) at the moment of reaching the Oort cloud. This shows that Neptune acts as a dynamical barrier, scattering most of the bodies to near-parabolic orbits before they can approach or cross Neptune's orbit in non-resonant orbits (that may allow their transfer to the planetary region as Centaurs via close encounters with Neptune). Consequently, Neptune's dynamical barrier greatly favors insertion in the Oort cloud at the expense of the other end states mentioned above. We found that the current rate of SDOs with radii $R > 1$ km incorporated into the Oort cloud is about 5 yr^{-1}, which might be a non-negligible fraction of comet losses from the Oort cloud (probably around or even above 10%). Therefore, we conclude that the Oort cloud may have experienced and may be even experiencing a significant renovation of its population, and that the trans-neptunian belt—via the scattered disk—may be the main feeding source.

© 2004 Elsevier Inc. All rights reserved.

Keywords: Edgeworth–Kuiper belt; Scattered disk; Oort cloud; Comets, dynamics

1. Introduction

Comets are considered to be the leftovers of planet formation. In particular, the Uranus–Neptune zone has been suggested as the source of most Oort cloud comets (e.g., Fernández, 1980a; Fernández and Ip, 1981). Yet, there are other potential sources of icy (cometary) bodies, that goes from the "snowline" in the protoplanetary disk, i.e., the region between 4–6 AU where water vapor condensed, to the trans-neptunian (TN), or Edgeworth–Kuiper (EK) belt at 40–50 AU. The latter region has been proposed as the source region of Jupiter family (JF) comets (Fernández, 1980b; Duncan et al., 1988, 1995). The delivery of comets from the TN belt to the inner planetary region requires the presence of a transient population of bodies whose orbits have been removed from the TN belt. This assertion was observationally confirmed with the discovery of the *Centaurs*, whose orbits lay in the region of the jovian planets, (2060) Chiron being the first of this class discovered in 1977 (Kowal, 1989). Levison and Duncan (1997) carried out extensive numerical integrations of bodies starting in Neptune-encountering orbits. They followed the evolution of the bodies for 1 Gyr, which allowed them to estimate the efficiency of transfer to JF orbits at about 30% of the original sample.

As well as there is a transient population scattered to the inner planetary region, it was also expected to find bodies scattered outwards on very eccentric orbits and with per-

---

* Corresponding author.
E-mail address: julio@fisica.edu.uy (J.A. Fernández).

ihelia around or beyond Neptune's orbit. The existence of such a population was observationally confirmed by the discovery of 1996 TL$_{66}$ (Luu et al., 1997). Within the growing complexity of the trans-neptunian population, this new class of bodies were called *Scattered Disk Objects* (SDOs). SDOs are usually defined as those with perihelion distances $q > 30$ AU and semimajor axes $a > 50$ AU. From numerical integrations over 4 byr, Duncan and Levison (1997) were able to reproduce such a scattered disk from TN objects (TNOs) strongly perturbed by close encounters with Neptune. The sample of discovered SDOs has risen to nearly 70 objects (end of 2002).

As more and more bodies are being discovered in the trans-neptunian region, a dynamical structure has emerged that shows different dynamical groupings. Jewitt et al. (1998) distinguish the following groups: (1) the *classical* belt composed of objects in non-resonant orbits with semimajor axes in the range 42 AU $\lesssim a \lesssim 48$ AU in low inclination and low eccentricity orbits; (2) objects in mean motion resonances with Neptune, the *Plutinos* in the 2:3 resonance being the most populous group. Objects in such resonances are prevented from having close encounters with Neptune; and (3) the *scattered disk* as described above. Figure 1 plots the different populations in the parametric plane semimajor axis vs. eccentricity.

A few of the discovered SDOs have perihelion distances $q > 38$ AU, i.e., they are well detached from the planetary region. The existence of such objects, that form an "Extended Scattered Disk" (ESD) (Gladman et al., 2002), seems difficult to explain as a result of the scattering process by gravitational interactions with Neptune (see also Emel'yanenko et al., 2003). We do not plan to discuss here whether such bodies derive from the trans-neptunian belt via diffusive chaos or another dynamical mechanism—as we assumed for

most of the SDOs—, or whether they constitute the "fossil" record of a primordial population, originally formed closer to the Sun, and then pushed out during Neptune's migration (Levison and Morbidelli, 2003). Such an extended scattered disk could be or could not be related to the scattered disk (whose bodies have $q < 38$ AU and are thus subject to Neptune's gravitational perturbations), but this point is not relevant for our study. Nevertheless, as a matter of completeness, we have computed the orbits of all SDOs, including those of the ESD.

The population of SDOs with radius $R > 50$ km has been estimated by Trujillo et al. (2000) at $(3.1^{+1.9}_{-1.3}) \times 10^4$ bodies (1σ errors) and the total mass at $0.05 M_\oplus$. Trujillo et al. considered the sample of four discovered SDOs at that time, which all had $q \leqslant 36$ AU. If we consider instead the SDOs up to $q = 40$ AU, Trujillo et al.'s estimate has to be multiplied by at least a factor of two. Therefore, in the following, we will adopt a SD population of $\sim 6 \times 10^4$ objects with $R > 50$ km. An independent survey conducted by Larsen et al. (2001) led to the discovery of 5 Centaurs/SDOs and other two recoveries. From this survey they estimate a population of 70 SDOs brighter than apparent red magnitude $m_R = 21.5$. Applying appropriate bias corrections for distance in the detection probability, the estimated total population is in good agreement with that derived above. Trujillo et al. (2001) find that the differential size distribution of classical TNOs follows a power-law of index $s = 4.0^{+0.6}_{-1.3}$ (1σ errors). If we assume that this size distribution also applies to SDOs and that the same exponent s holds down to a typical comet radius $R = 1$ km, the total population of SDOs is estimated to be

$$N_{\text{SDO}}(R > 1 \text{ km}) = 6 \times 10^4 \times 50^{(s-1)}. \qquad (1)$$

Taking $s = 4.0$ as the most likely value, we obtain $N_{\text{SDO}} = 7.5 \times 10^9$, but it may go up to (within 1σ) 7.8×10^{10}, or down to 1.1×10^9 bodies for $s = 4.6$ and 3.5, respectively. Therefore, there is an uncertainty of an order of magnitude in the estimated SD population. A recent deep survey with the HST/ACS camera carried out by Bernstein et al. (2004) hints at a smaller population of small TNOs than that predicted by an extrapolation of a power-law of index $s = 4.0$. Duncan and Levison (1997) estimate that $\sim 6 \times 10^8$ SDOs could supply all the observed JF comets, though this result might be model-dependent and actually represent a lower limit. This is because they start with a sample of test particles already in Neptune-encountering orbits, while a large fraction of the SDOs have perihelia well above Neptune.

We shall adopt in the following a canonical value for the SD population of 7.5×10^9 objects, though one should bear in mind that it is still very uncertain and it could be one order of magnitude greater or smaller. Since SDOs can diffuse either to the planetary region or to large heliocentric distances, it may also be a potential source of Oort cloud comets. This point is what we plan to analyze in this paper.
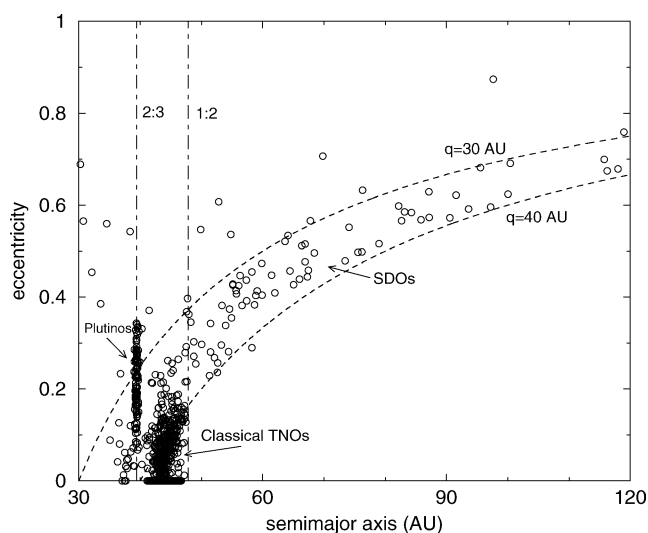

Fig. 1. Distribution of the different populations of trans-neptunian bodies in the plane a–e. The objects were taken from the Minor Planet Center's Web site: http://cfa-www.harvard.edu/iau/Ephemerides/Distant/Soft00Distant.txt.

2. The numerical model

We integrated numerically the orbits of 76 SDOs (that included a few objects with $q < 30$ AU) taken from the Minor Planet Center's Web site: http://cfa-www.harvard.edu/iau/Ephemerides/Distant/Soft00Distant.txt (the list corresponds to the end of 2002). Some preliminary results of these integrations were already published elsewhere (Fernández et al., 2004). Since the sample of real objects was considered to be too small, we added to our integrations 399 clones with the same orbits as the real objects, but with different initial positions in their orbits (i.e., different initial mean longitudes). The number of clones for each real SDO was chosen in order to approximately account for the bias in the discovery probability for different semimajor axes, namely comets with large semimajor axes spend relatively less time near perihelion where they can be discovered, so they should represent more objects.

The numerical integration was performed with our numerical code EVORB that consists of a mixed-variable leap-frog integrator, inspired by the Wisdom and Holman (1991) symplectic map. Our code is not a fully symplectic integrator because every close encounter between a test body and a planet (considered as those within three Hill radii) is computed by means of a Bulirsch–Stoer routine. In addition, the integration is always performed in a heliocentric reference frame. However, for the computation of the orbital elements we transfer the origin to a barycentric frame. A report about the accuracy of the integrator can be found in Fernández et al. (2002).

The dynamical model developed here included the Sun and the four giant planets, while the masses of the terrestrial planets were added to that of the Sun. We used an integration step of 0.25 yr. The test bodies (real SDOs + clones) were assumed to be massless. They were integrated for 5 Gyr, but the integration was terminated if one of the following end states was reached:

1. Collision onto a planet.
2. Arrival to the region interior to Jupiter's orbit ($r < 5.2$ AU), in which case the body could be either ejected or transferred to a JF comet orbit in a very short time scale.
3. Attaining a distance of 20,000 AU from the Sun still in a barycentric elliptical orbit. In this case we considered that the body was stored in the Oort cloud. This assumption is justified on the basis that passing stars and the tidal force of the galactic disk are able to raise the perihelia of the SDOs at such near-interstellar distances well beyond the dynamical influence of the planets (e.g., Fernández and Ip, 1991; Dybczyński, 2001).
4. Attaining a distance of 20,000 AU from the Sun in a barycentric hyperbolic orbit. In this case we considered that the body was ejected to interstellar space.
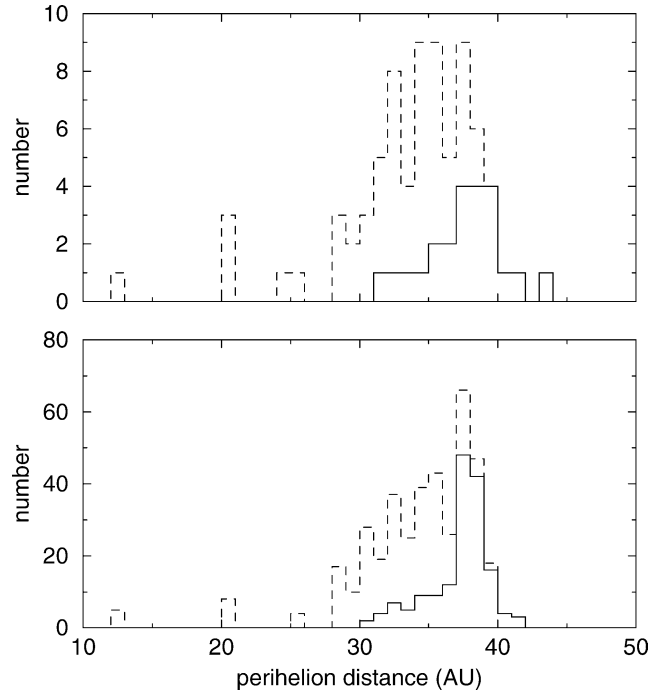

Fig. 2. (Top) Initial sample of real SDOs (dashed histogram) and survivors after 5 Gyr (solid histogram) distributed according to their initial perihelion distances. (Bottom) The same as before but for the sample of clones.

3. The results

3.1. Dynamical lifetimes of SDOs

The survival of SDOs is a strong function of their initial perihelion distance. This is evident when we compared the sample of real objects and the clones at the beginnings of the integration with that remaining at the end, distributed according to their initial perihelion distances (Fig. 2). It is shown that most of the SDOs whose initial perihelion distances are $q_i \lesssim 36$ AU are lost at the end of the studied period. On the other hand, most of the bodies remain for $q_i \gtrsim 38$ AU after 5 Gyr, which gives some support to the idea that they form a special extended disk, perhaps with a different origin (see Section 1).

The results shown in Fig. 2 can be described in a more quantitative way in Fig. 3 where the dynamical half-life is plotted as a function of the initial perihelion distance. For the purpose of these computations we divided the overall sample of real SDOs plus clones in sub-samples within ranges of perihelion distances of 2 AU, starting at 30 AU. For these sub-samples we computed the dynamical half-life, i.e., the time it requires the sample to decrease to a half. We can fit an empirical linear relation between the dynamical half-life and the initial perihelion distance q_i as follows

$$\log t_{\mathrm{dyn}} = a + bq_i, \tag{2}$$

where $a \simeq 1.857$ and $b \simeq 0.213$. We can express Eq. (2) in a more convenient way as

$$t_{\mathrm{dyn}} = 10^{\frac{(q-33.5)}{4.7}} \ \mathrm{Gyr}, \tag{3}$$
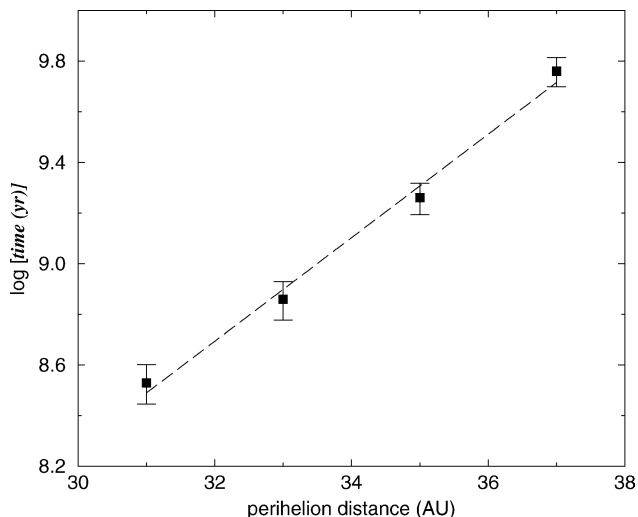
Fig. 3. Dynamical half-lives of SDOs and their clones as a function of their initial perihelion distances.

where q is expressed in AU. From Eq. (3) we can see that objects with $q \gtrsim 36.6$ AU already have dynamical half-lives that exceed the Solar System age.

We can compute the average dynamical half-time $\bar{t}_{\mathrm{dyn}}$ for the region just beyond Neptune's orbit (say for initial perihelion distances 31 AU $< q_i <$ 36 AU) as

$$\bar{t}_{\mathrm{dyn}} = \frac{\int_{t_1}^{t_2} t_{\mathrm{dyn}} \, dt_{\mathrm{dyn}}}{\int_{t_1}^{t_2} dt_{\mathrm{dyn}}} = \frac{\int_{q_1}^{q_2} [t_{\mathrm{dyn}}(q_i)]^2 b \ln 10 \, f_q(q_i) \, dq_i}{\int_{q_1}^{q_2} t_{\mathrm{dyn}}(q_i) b \ln 10 \, f_q(q_i) \, dq_i}, \quad (4)$$

where $q_2 = 36$ AU and $q_1 = 31$ AU, and $f_q(q_i) \, dq_i$ is the fraction of SDOs with initial perihelion distances $(q_i, q_i + dq_i)$ with respect to those in the interval 31 AU $< q_i <$ 36 AU. In the following, we consider $f_q(q_i)$ uniform in the previous interval, which simplifies the computations and, we believe, does not introduce a large error with respect to the use of other possible distributions. Furthermore, we have from Eq. (2): $dt_{\mathrm{dyn}}/t_{\mathrm{dyn}} = \ln 10 \, b \, dq_i$.

By integrating Eq. (4) and substituting the corresponding numerical values we obtain

$$\bar{t}_{\mathrm{dyn}} = 1.8 \times 10^9 \text{ yr.}$$

3.2. The different end states

From the 76 real SDOs, 53 were lost at the end of the studied period with the following end states: 26 were placed into the Oort cloud, 12 were ejected to interstellar space, and 15 reached Jupiter's region. That gives the following fractions among the lost objects: $f_{\mathrm{Oort}} = 26/53 = 0.49 \pm 0.10$, $f_{\mathrm{hyp}} = 12/53 = 0.23 \pm 0.06$, and $f_{\mathrm{jup}} = 15/53 = 0.28 \pm 0.07$. The respective values for the clones were: 239 were lost from the initial 399 bodies with the following percentages $f_{\mathrm{Oort}} = 0.46 \pm 0.044$, $f_{\mathrm{hyp}} = 0.26 \pm 0.033$, and $f_{\mathrm{jup}} = 0.28 \pm 0.034$. The results are thus very similar. By combining both samples, we obtain

$$f_{\mathrm{Oort}} = 0.47 \pm 0.04,$$
$$f_{\mathrm{hyp}} = 0.25 \pm 0.029,$$
$$f_{\mathrm{jup}} = 0.28 \pm 0.031.$$

Therefore, nearly half of the bodies that are lost go to the Oort cloud. The other half are more or less evenly split between those ejected on hyperbolic orbits and those that reach Jupiter's orbit.

3.3. Capture into resonant states

We elaborated a simple program to automatically detect objects that stay or fall in mean motion resonances during their dynamical evolution. For each object the program computes the critical angles for several mean motion resonances. If a specific critical angle shows a nonuniform distribution between 0° and 360°, the program looks at the semimajor axis of the body's orbit. In case it is close to the theoretical value of the resonance corresponding to this critical angle, it will be indicated as a potential resonance. We can then confirm it by visual inspection of the time evolution of the critical angle. We applied this program to the real SDOs and could detect several mean motion resonances with Neptune that are shown in Table 1. As shown in the table, the 2:5, 3:7, and 4:9 resonances are found to be very stable orbital states, even for high eccentricities such as those

Table 1
Resonant states

| Object	Resonance	a (AU)	e	Time spent in the resonance (Gyr)
2002 CZ$_{248}$	1:2	47.6	0.25	0.7
2000 SS$_{331}$	1:3	62.4	0.51	At the beginning (0.08)
2001 KV$_{76}$	1:3	62.4	0.41	At the beginning (2.0)
1999 RZ$_{215}$	1:5	87.7	0.60	0.1
2002 GB$_{32}$	1:6	99.1	0.61	At the beginning (0.5)
2001 FP$_{185}$	1:13	166.3	0.74	1.0
2000 SR$_{331}$	2:5	55.3	0.43	All
2000 FE$_{8}$	2:5	55.3	0.40	All
2001 KC$_{77}$	2:5	55.3	0.33	All
1999 DG$_{8}$	2:9	81.8	0.51	At the beginning (1.5)
1999 HW$_{11}$	3:7	52.8	0.30	All
1999 CV$_{118}$	3:7	52.8	0.30	2.7
2001 KG$_{76}$	4:9	51.5	0.34	All
2001 QW$_{297}$	4:9	51.5	0.25	All
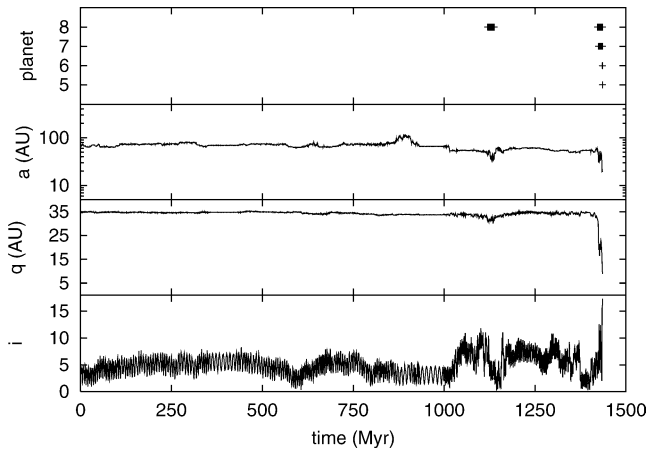
Fig. 4. Dynamical evolution of the SDO 2002 GY$_{32}$ that ends up in Jupiter's zone. Close encounters with any of the jovian planets are indicated in the upper panel, where the numbers 5 ... 8 stand for Jupiter...Neptune, respectively.

for 2000 SR$_{331}$ and 2000 FE$_8$ that are above or around $e = 0.4$.

3.4. Dynamical evolution of some particular SDOs

We illustrate in the following a few interesting examples of real SDOs that have different end states. Object 2000 GY$_{32}$ ended up in Jupiter's region (Fig. 4). For a little more than 1 Gyr its evolution is very smooth because it has its perihelion well outside Neptune's orbit that prevents it from suffering strong perturbations. Afterwards, the body decreases its q which allows it to have a few close encounters with Neptune. The decrease in q is accompanied by a decrease in its semimajor axis a. Yet, the values of q and a return to more or less the previous values, so the body is spared from having new close encounters with Neptune for the next ~ 300 Myr. At $t \sim 1.4$ Gyr its q drops again, so close encounters with Neptune occur again. In one of the close encounters the body is handed down to Uranus, and the dynamical process repeats itself, the body is handed down to the next planet inside, Saturn, and finally Jupiter. Therefore, at the very end of its evolution the object becomes a Centaur before it falls under the gravitational control of Jupiter. The transfer from Neptune to Jupiter is very fast in cosmogonic terms: it takes not more than a few Myr.

Object 1999 DG$_8$ keeps a perihelion distance oscillating between ~ 32–42 AU while its semimajor axis remains nearly constant during a little more than 1.5 Gyr because it is locked in the 2:9 mean-motion resonance with Neptune, as can be seen by the libration of its critical angle around 180° (Fig. 5). This resonance prevents the object from having close encounters with this planet. The Kozai mechanism also acts together with the 2:9 resonance forcing coupled oscillations in the perihelion distance and inclination. Afterwards it leaves the resonance so close encounters with Neptune become frequent. The body's perihelion penetrates within the planetary region, where it also suffers a few close
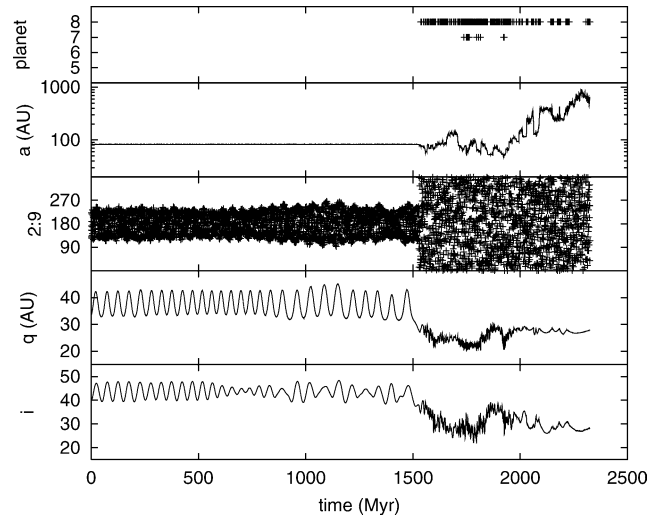

Fig. 5. Dynamical evolution of the SDO 1999 DG$_8$ that ends up ejected in a hyperbolic orbit.
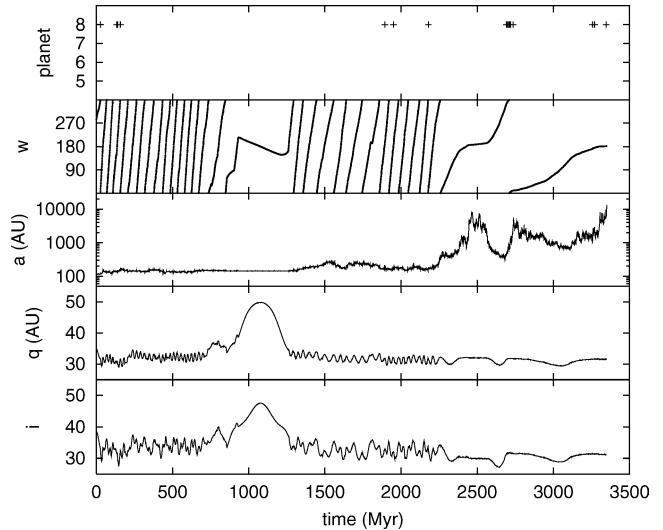

Fig. 6. Dynamical evolution of the SDO 1999 DP$_8$ that ends up in the Oort cloud.

encounters with Uranus. Once the body leaves the resonance its semimajor axis starts to random-walk until the body is ejected to interstellar space.

Object 1998 DP$_8$ ends up in the Oort cloud after 3.35 Gyr (Fig. 6). The Kozai mechanism acts on the body for a time during which its perihelion distance rises to ~ 50 AU and its inclination also increases. We can see that the argument of perihelion ω stops circulating and librates around 180°. We found that the Kozai mechanism plays a very important dynamical role in the evolution of SDOs, but its detailed study exceeds the scope of this paper. It will be analyzed in a forthcoming publication. Once the Kozai mechanism stops acting on the body, its q returns to the previous level. The evolution is not longer adiabatic and the semimajor axis random walks until reaching the Oort cloud.

Object 2001 FN$_{194}$ also ends up in the Oort cloud after 2.27 Gyr (Fig. 7). It is interesting to note that its perihe-
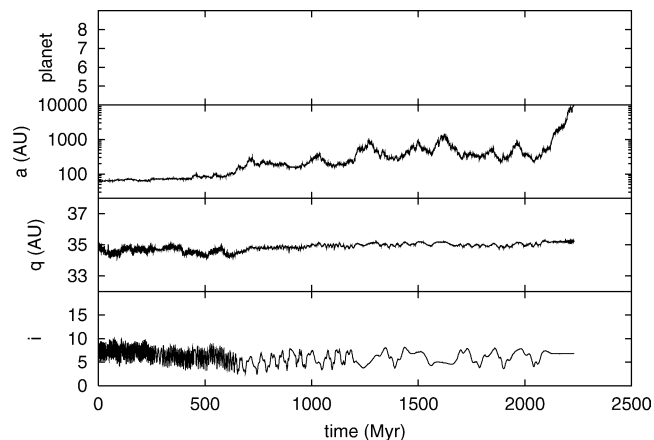
Fig. 7. Dynamical evolution of the SDO 2001 FN$_{194}$ that ends up in the Oort cloud.
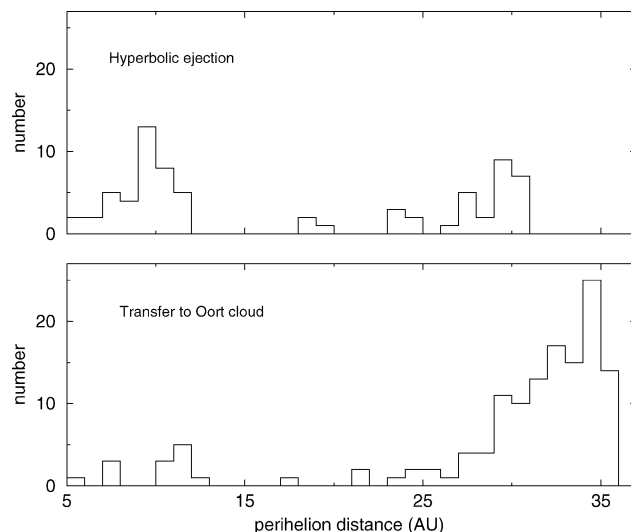

Fig. 8. The distribution of perihelion distances of the total sample of objects (real SDOs + clones) at the moment they reach their final state: hyperbolic ejection (top), or insertion in the Oort cloud (bottom).
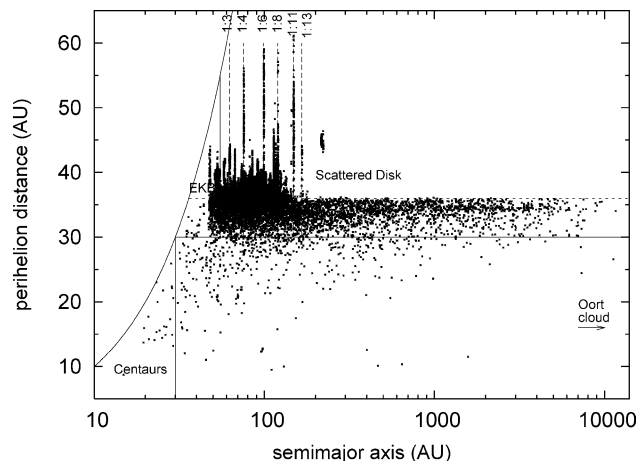

Fig. 9. Perihelion distance versus semimajor axis of all the objects (real SDOs + clones) plotted every 50 Myr.

lion distance never decreases below 34 AU, so there are not close encounters with Neptune during its evolution. Nevertheless, gravitational perturbations by the distant Neptune (and the other jovian planets) are strong enough to diffuse the body's semimajor axis until it reaches the Oort cloud. We shall come back to this point in the next section.

4. The Neptune dynamical barrier

As shown in Section 3.2, the scattered disk is a very efficient route to the Oort cloud. A close inspection into the dynamics of SDOs reaching the Oort cloud permits us to verify the following interesting property: A large fraction of the SDOs reaching the Oort cloud have their perihelia *beyond* Neptune's orbit, and most of them never crossed Neptune's orbit (see example of Fig. 7). We found that Neptune acts as a *dynamical barrier* that scatters bodies approaching the planet from outside to larger semimajor axes, before their perihelia can enter Neptune's orbit. Actually, among the 137 objects that end up in the Oort cloud (real SDOs + clones), 85 have perihelion distances in the range 31 AU < q < 36 AU at the moment of reaching the Oort cloud, that gives a fraction 0.62 ± 0.067.

Figure 8 shows the distribution of perihelion distances of the bodies at the moment they reach their final states. For those bodies that cross the orbit of one or more jovian planets, hyperbolic ejection is found to be a much more likely outcome than insertion in the Oort cloud. This can be understood bearing in mind that planetary perturbations become much stronger once the bodies enter the planetary region, that entails besides the frequent occurrence of close encounters with the planets. Consequently, the strong energy kicks imparted by the planets make the bodies in their random-walk in the energy space more likely to overshoot the narrow energy range corresponding to the Oort cloud straight to interstellar space, rather than to fall into it.

The main dynamical features of the diffusion of SDOs to the Oort cloud can also be illustrated in the paramet-

ric plane (a, q) (Fig. 9). Positions of the bodies are plotted every 50 Myr. We can see that most of the SDOs evolve to the Oort cloud in the lane 31 AU < q < 36 AU (see also Fig. 8). No SDO evolves to the Oort cloud with q > 36 AU, which shows that it must first decrease its q and then diffuse in a, result that was already shown by Holman and Wisdom (1993).

We can analyze the previous condition by considering the energy change per orbital revolution as due to planetary perturbations (see, e.g., Fernández and Brunini, 2000). We recall that the orbital energy $E = -GM_\odot/2a$, so we can adopt $x = 1/a$ as the orbital "energy" since it is proportional to E. We define the typical energy change ϵ_x as the standard deviation of the distribution of energy changes Δx, obtained from samples of N test bodies of (high) eccentricity e within certain ranges of perihelion distances and inclinations, and with random argument of perihelion ω and longitude of ascending node Ω, thus we have
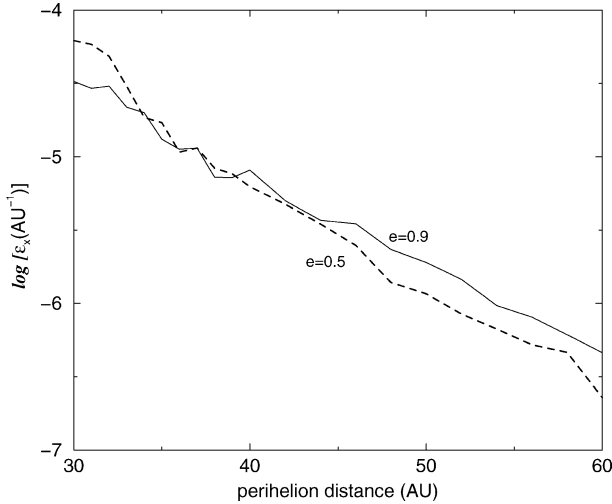
Fig. 10. The typical energy change per orbital revolution of samples of highly eccentric orbits ($e = 0.9$) and moderately eccentric orbits ($e = 0.5$), with inclinations in the range $0° < i < 5°$. Every point was computed with a sample of 100 test particles with perihelion distances within a bin of one AU.

$$\epsilon_x^2 = \sum_{i=1}^{N} \frac{\Delta x_i^2}{N}, \tag{5}$$

where the mean of the Δx-distribution is zero.

We show in Fig. 10 the typical energy change ϵ_x per orbital revolution for bodies in low-inclination ($0° < i < 5°$), highly eccentric orbits ($e = 0.9$) computed from Eq. (5). Each point was computed with a sample of $N = 100$ bodies within q ranges of 1 AU. We also show the computed ϵ_x for samples with the same conditions as the previous ones, but less eccentric orbits ($e = 0.5$), which are typical of SDOs. We can see that the values do not differ too much, except for q close to Neptune's orbit where ϵ_x is about a factor of two higher than that for orbits with $e = 0.9$. We also computed ϵ_x for higher inclinations ($5° < i < 10°$), but the results are not very different from those for ($0° < i < 5°$). We find that ϵ_x drops by nearly two orders of magnitude for perihelion distances between 30 and 60 AU, which shows the rapidly diminishing influence of planetary perturbations in the trans-neptunian region.

We can roughly estimate the average number of revolutions N that a body with a perihelion distance $q \sim 32$ AU requires to reach the Oort cloud starting in an orbit in the scattered disk with a semimajor axis $a = 50$ AU, assuming that it random walks in energy. In this case we have

$$N \simeq \left(\frac{1/a_{\text{init}}}{\epsilon_x} \right)^2. \tag{6}$$

If we adopt $\epsilon_x \simeq 4 \times 10^{-5}$ AU^{-1} as typical for bodies with $q = 32$ AU, we obtain

$$N \simeq \left(\frac{0.02}{4 \times 10^{-5}} \right)^2 = 2.5 \times 10^5 \text{ revolutions.}$$

If we now adopt an average orbital period of 10^4 yr, we get a dynamical lifetime to reach the Oort cloud of 2.5×10^9 yr,

which is in reasonable agreement with the value found in Section 3.1. Yet, for $q = 38$ AU the typical energy change decreases to $\epsilon_x \simeq 10^{-5}$ AU^{-1}, so the time scale to reach the Oort cloud raises to 4×10^6 revolutions, or 4×10^{10} yr, i.e., an order of magnitude longer than the Solar System lifetime. It is then clear that bodies with $q \sim 38$ AU will first have to decrease their perihelia to diffuse to the Oort cloud over time scales comparable to the Solar System age, in agreement with what was found in Fig. 9. We note that Eq. (6) is not totally correct since the diffusion from a semimajor axis so small (50 AU) is not really a random walk. In other words, for small a the body keeps "memory" of the previous planetary configuration, and this is particularly the cases of bodies that are located in mean motion resonances for different periods of time (see Fig. 9). The highest resonance we found is 1:13 that corresponds to a semimajor axis $a \sim 166.3$ AU. We can thus say that only for $a \gtrsim 166$ AU, the scattering of a corresponds to a random walk.

5. The dependence of the end state on the initial perihelion distance

Two possible sources have been suggested for the scattered disk: (1) a primordial origin, in which the current SD would be the fossil record of the early massive scattering of planetesimals by the accreting Neptune (Duncan and Levison, 1997); and (2) the trans-neptunian belt that feeds the SD via chaotic diffusion (e.g., Holman and Wisdom, 1993; Morbidelli, 1997). In the latter case, the most likely source regions are the 2:3 mean motion resonance (Plutinos), and the classical belt in the range 40–42 AU where there is an overlapping of several secular resonances. In both cases bodies tend to increase their eccentricities, while keeping their semimajor axes nearly constant, until they get close to Neptune's orbit. This is certainly a dynamical process that works and warrants a dynamical link between SDOs and Plutinos and classical TNOs. It seems then reasonable to assume that the SD population is currently being replenished by Plutinos and classical TNOs, and that the primordial population, if it still remains any, forms only an unknown fraction of the total.

It has been shown in Section 4 (cf. Fig. 8) that bodies whose perihelia are close to or cross Neptune's orbit ($q \lesssim 31$ AU) have more chances to be transferred to the planetary region or being ejected hyperbolically, in other words, these are the bodies that penetrate the Neptune's barrier. Therefore, the end states of the SDOs should depend somewhat on the distance (from Neptune's orbit) at which they were decoupled from their resonances and started to diffuse in semimajor axes until becoming SDOs when $a > 50$ AU. In Fig. 11 we show the fraction of bodies that reach Jupiter's zone with respect to all the bodies that reach the different end states (namely, Jupiter's zone + hyperbolic ejection + Oort cloud), as a function of the initial perihelion distance. We can see that about 1/3 of the SDOs initially close to Nep-
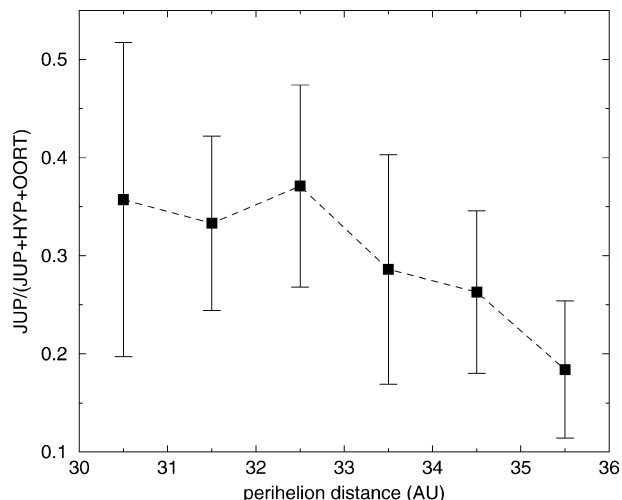
Fig. 11. The ratio of SDOs that end up in Jupiter's zone to the total SDOs lost in the different end states (Jupiter's zone, hyperbolic ejection, Oort cloud) as a function of the initial perihelion distance. The plotted values represent averages within one-AU bins.

tune's orbit (30 AU $< q <$ 32 AU) end up in Jupiter's zone, a fraction that is in agreement with that found by Levison and Duncan (1997). Yet, for SDOs starting their evolution with larger q, the fraction transferred to Jupiter's zone drops at the expense of the increase in the fraction of SDOs that reach the Oort cloud. The explanation for this behavior is that such bodies, initially farther from Neptune's orbit, meet more serious difficulties to penetrate Neptune's barrier, an indispensable condition to be handed down to Uranus, Saturn, and finally Jupiter. In other words, to be transferred to the planetary region, the body must have its perihelion close to Neptune's orbit and have decreased its eccentricity to a near circular orbit, so its perihelion can be flipped to the aphelion of the new orbit (that falls within the planetary region) after a close encounter with Neptune (Morbidelli, 1999).

As shown by Morbidelli (1997), a body can be decoupled from the 2:3 resonance with different eccentricities. For instance, if $e = 0.1$, the body will be decoupled with an initial $q = 35.6$ AU, for $e = 0.2$ with $q = 31.6$ AU, and for $e = 0.3$ with $q = 27.6$ AU, namely there is a wide range of initial perihelion distances, including Neptune-crossing orbits, with which the bodies can be left before starting their evolution in the scattered disk. As said above, the outcome will be different in these three cases. For the first body transfer to the Oort cloud will be the most likely outcome, while the second and third bodies will have a greater probability of reaching Jupiter's region. In the third case hyperbolic ejection becomes about as likely as insertion in the Oort cloud.

6. The transfer rate of SDOs to the Oort cloud

From our computed results we can make a rough estimate of the rate of SDOs injected in the Oort cloud from
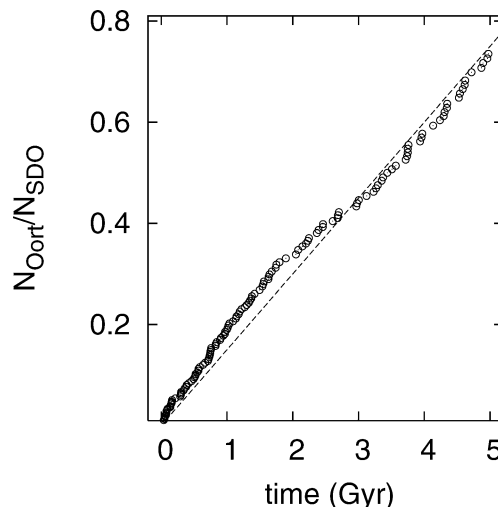

Fig. 12. The ratio of the cumulative number of SDOs incorporated into the Oort cloud over the remaining SDO population as a function of time.

the *current* scattered disk population: $N_{\text{SDO}} = 7.5 \times 10^9$ (for $R > 1$ km). This is an important point to stress, since we computed the orbits to the future, and thus the computed rate will correspond to the time when the currently observed SDOs reach the Oort cloud. We found that about 60% of the SDOs are lost after 5 Gyr. If we then assume that this fraction of N_{SDO} bodies with radius > 1 km are lost, and that $f \sim 0.5$ of them end up in the Oort cloud on an average time scale of $\bar{t}_{\text{dyn}} \sim 1.8 \times 10^9$ yr (cf. Section 3.1), then the injection rate ν will be

$$\nu = \frac{N_{\text{SDO}} \times 0.6 \times f}{\bar{t}_{\text{dyn}}} = 1.2 \text{ yr}^{-1}. \tag{7}$$

As said before, this is actually the injection rate in the *future* (within ~ 1.8 Gyr) from the scattered disk population observed at *present*.

We can compare the rate ν, obtained from Eq. (7), with an independent estimate from an empirical law that describes how the ratio $N_{\text{Oort}}/N_{\text{SDO}}$ varies with time t, where N_{Oort} is the cumulative number of SDOs transferred to the Oort cloud at time t, and N_{SDO} is the remaining population of SDOs at t. As Fig. 12 shows, the ratio $N_{\text{Oort}}/N_{\text{SDO}}$ is well fitted by a linear relation, namely

$$N_{\text{Oort}} = 1.5 \times 10^{-10} \times N_{\text{SDO}} \times t, \tag{8}$$

where t is expressed in years.

The simplest case is to assume that N_{SDO} is constant with t. If we thus take $N_{\text{SDO}} = 8 \times 10^9$, the injection rate of SDOs into the Oort cloud is

$$\nu = \frac{d N_{\text{SDO}}}{dt} = 1.5 \times 10^{-10} \times N_{\text{SDO}}$$
$$= 1.5 \times 10^{-10} \times 8 \times 10^9 = 1.2 \text{ yr}^{-1}, \tag{9}$$

which agrees with the result obtained from Eq. (7).

We would like to know how the population of SDOs varies with time. We have very few clues to learn about this

problem. We may conjecture that the trans-neptunian population was much more massive at the beginning than it is now, perhaps by a factor of 100, based on cosmogonic reasons, as well as on estimates of the amount of mass required to form 100-km to 1000-km class bodies (Stern, 1995; Stern and Colwell, 1997). The original scattered disk population would have been correspondingly as massive as the trans-neptunian belt population, so we can adopt a law

$$dN = -\frac{N}{\tau} dt, \tag{10}$$

where τ is the dynamical lifetime of bodies in the scattered disk. We note that τ does not necessarily corresponds to the value of $\bar{t}_{dyn}$ computed from Eq. (4), since the latter was derived for the *current* population of SDOs with a certain distribution of perihelion distances that may vary with time. This means that τ may be somewhat a function of time, though in the following we will take it constant for a matter of simplicity. Equation (10) upon integration leads to

$$N_{SDO} = N_o \exp\left(-\frac{t}{\tau}\right), \tag{11}$$

where N_o is the original population of the scattered disk.

If, as argued above, we take the original SD population as 100 times the current one, then we have $N_{SDO}(T) = N_o/100$, where $T = 4.6 \times 10^9$ yr. By introducing this value in Eq. (11) we obtain

$$\tau = \frac{T}{\ln(N_o/N_{SDO})} = \frac{4.6 \times 10^9}{\ln 100} \simeq 10^9 \text{ yr.} \tag{12}$$

We find that τ is somewhat smaller than $\bar{t}_{dyn}$, which makes sense if we consider that the primordial SD population may have had a predominance of bodies with shorter dynamical lifetimes, that are by now practically gone.

From Eq. (11) we can say that the SD population about 1.8 Gyr ago was $N_{SDO} \sim N_o \exp[-(4.6-1.8) \times 10^9/10^9] \sim 100 \times 7.5 \times 10^9 \times \exp(-2.8) \sim 4.6 \times 10^{10}$, i.e., about 6 times greater than at present. This result can be compared with those derived from the numerical simulations of Duncan and Levison (1997). They found that the original population of test bodies decreases to 5 percent after 1 Gyr and to 1 percent after 4 Gyr. This would give a decrease by a factor 2–3 between 2.8 and 4.6 Gyr. Again we note some differences in their model, since they start with a sample of test bodies with semimajor axes between 34 and 50 AU, while SDOs are defined as those with $a > 50$ AU. What we can say from this discussion is that the SD population 1.8 Gyr ago probably was a few times greater than at present, say ~ 4 with an uncertainty of 50%.

According to the previous discussion, a SD population $\sim 7.5 \times 10^9 \times 4 = 3 \times 10^{10}$ is the one that provides the *current* injection rate of SDOs into the Oort cloud. Thus we have

$$\nu \simeq 5 \text{ yr}^{-1}.$$

The average rate $\bar{\nu}$ over the age of the Solar System should be greater bearing in mind that the primordial SD population could have been up to 10^2 times greater, so a value $\bar{\nu} \sim 10$ should give at least the correct order of magnitude. Adopting this value, we get for the total number of SDOs incorporated into the Oort cloud $N_{Oort} \sim 4.6 \times 10^9 \times 10 = 4.6 \times 10^{10}$. This result shows that the trans-neptunian belt (via the scattered disk) could have been a major supplier of bodies to the cloud, even rivaling other sources within the planetary region, as for instance the Uranus–Neptune zone.

7. Discussion

We can compare the previous result for the injection rate ν of SDOs into the Oort cloud with current comet losses from the Oort cloud. Comets are lost from the Oort cloud mainly because they are injected into the inner part of the planetary region where Jupiter and Saturn exert the greatest perturbing influence, say within ~ 15 AU to the Sun (e.g., Fernández, 2002). The passage rate of new comets in Earth-crossing orbits and radius $R > 1$ km is found to be about one every two years, so if we adopt a loss cone of 15 AU, then by simply extrapolation up to 15 AU we would obtain a passage rate of $\sim 7.5 \text{ yr}^{-1}$. Yet this is clearly a lower limit, since the passage rate of new comets increases with q in an as yet unknown manner. A reasonable guess is to assume that the passage rate of new comets with $q < 15$ AU and $R > 1$ km should be on the order of a few tens per year. Therefore, the injection rate of SDOs into the Oort cloud might represent a non-negligible fraction of the comet losses from the cloud, probably around or even above 10%, so we can argue that the Oort cloud is experiencing a non-negligible renovation of its population, not only from a putative inner core, but also from a population nearer home, as it is the case of the SD (and thus of the trans-neptunian belt if it is its source).

The previous discussion has important consequences for the chemical nature of comets. If some—or most—Oort cloud comets as well as JF comets come from the trans-neptunian belt, then both populations should show chemical similitudes among some of their members, at least in their deep interiors, which should indicate very low condensation temperatures of the cometary material. The comet nuclei of new and JF comets may nevertheless show differences at the surface level, because of the different exposures to cosmic rays and solar radiation.

8. Conclusions

We can then summarize our most important results as follows:

1. SDOs are lost on a dynamical time scale of $10^{\frac{(q-33.5 \text{ AU})}{4.7 \text{ AU}}}$ Gyr. About 50% of the lost SDOs go to the Oort cloud, the rest are ejected to interstellar space or reach Jupiter's influence zone.

2. Neptune acts as a dynamical barrier for SDOs whose perihelia are approaching Neptune's orbit, in such a way

that most of them diffuse in the energy space to the Oort cloud before crossing or approaching Neptune's orbit, and then have the chance to experience close encounters with this planet. We find that about 60% of the bodies inserted in the Oort cloud have perihelia beyond Neptune (31 AU < q < 36 AU) at the time of insertion. Close encounters with Neptune will favor orbit transfer to the planetary region (via flipping of the perihelion into the aphelion of the new orbit within the planetary region), or hyperbolic ejection, with a consequent decrease in the fraction transferred to the Oort cloud.

3. No SDOs are found to evolve to the Oort cloud while their perihelion distances are above $q \simeq 36$ AU. The reason is that the diffusion time to the Oort cloud by planetary perturbations becomes much longer than the Solar System age. Such bodies must first decrease its q and then evolve in a.

4. The current rate of SDOs injected into the Oort cloud is found to be ~ 5 yr^{-1}, which turns out to be a non-negligible fraction of comet losses from the Oort cloud (probably around or even above 10%). Consequently, the scattered disk (and then the trans-neptunian belt if it is the source of SDOs) may be an important source of Oort cloud comets even at present.

5. During the dynamical evolution some SDOs raise their perihelia to values ~ 50 AU or even greater, basically due to the Kozai mechanism. This is an interesting dynamical effect that deserves further exploration, currently in progress.

Acknowledgments

References

Bernstein, G.M., Trilling, D.E., Allen, R.L., Brown, M.E., Holman, M.J., Malhotra, R., 2004. The size distribution of transneptunian bodies. Astron. J. 128, 1364–1390.

Duncan, M.J., Levison, H.F., 1997. A disk of scattered icy objects and the origin of Jupiter-family comets. Science 276, 1670–1672.

Duncan, M., Quinn, T., Tremaine, S., 1988. The origin of short-period comets. Astrophys. J. 328, L69–L73.

Duncan, M.J., Levison, H.F., Budd, S.M., 1995. The dynamical structure of the Kuiper belt. Astron. J. 110, 3073–3081.

Dybczyński, P.A., 2001. Dynamical history of the observed long-period comets. Astron. Astrophys. 375, 643–650.

Emel'yanenko, V.V., Asher, D.J., Bailey, M.E., 2003. A new class of trans-neptunian objects in high-eccentricity orbits. Mon. Not. R. Astron. Soc. 338, 443–451.

Fernández, J.A., 1980a. Evolution of comet orbits under the perturbing influence of the giant planets and nearby stars. Icarus 42, 406–421.

Fernández, J.A., 1980b. On the existence of a comet belt beyond Neptune. Mon. Not. R. Astron. Soc. 192, 481–491.

Fernández, J.A., 2002. Long-period comets and the Oort cloud. Earth Moon Planets 89, 325–343.

Fernández, J.A., Brunini, A., 2000. The buildup of a tightly bound comet cloud around an early Sun immersed in a dense galactic environment: numerical experiments. Icarus 145, 580–590.

Fernández, J.A., Ip, W.-H., 1981. Dynamical evolution of a cometary swarm in the outer planetary region. Icarus 47, 470–479.

Fernández, J.A., Ip, W.-H., 1991. Statistical and evolutionary aspects of cometary orbits. In: Newburn Jr., R.L., Neugebauer, M., Rahe, J. (Eds.), Comets in the Post-Halley Era. Kluwer, Dordrecht, The Netherlands, pp. 487–535.

Fernández, J.A., Gallardo, T., Brunini, A., 2002. Are there many inactive Jupiter family comets among the near-Earth asteroid population? Icarus 159, 358–368.

Fernández, J.A., Gallardo, T., Brunini, A., 2004. The scattered disk population and the Oort cloud. Earth Moon Planets. In press.

Gladman, B., Holman, M., Grav, T., Kavelaars, J., Nicholson, P., Aksnes, K., Petit, J.-M., 2002. Evidence for an extended scattered disk. Icarus 157, 269–279.

Holman, M.J., Wisdom, J., 1993. Dynamical stability in the outer Solar System and the delivery of short period comets. Astron. J. 105, 1987–1999.

Jewitt, D.G., Luu, J., Trujillo, C., 1998. Large Kuiper belt objects: the Mauna Kea 8K CCD survey. Astron. J. 115, 2125–2135.

Kowal, C., 1989. A Solar System survey. Icarus 77, 118–123.

Larsen, J.A., Gleason, A.E., Danzi, N.M., Descour, A.S., McMillan, R.S., Gehrels, T., Jedicke, R., Montani, J.L., Scotti, J.V., 2001. The Spacewatch wide-area survey for bright Centaurs and trans-neptunian objects. Astron. J. 121, 562–579.

Levison, H.F., Duncan, M.J., 1997. From the Kuiper belt to Jupiter-family comets: the spatial distribution of ecliptic comets. Icarus 127, 13–32.

Levison, H.F., Morbidelli, A., 2003. Forming the Kuiper belt by the outward transport of objects during Neptune's migration. Nature 426, 419–421.

Luu, J., Marsden, B.G., Jewitt, D., Trujillo, C.A., Hergenrother, C.W., Chen, J., Offutt, W.B., 1997. A new dynamical class of object in the outer Solar System. Nature 387, 573–575.

Morbidelli, A., 1997. Chaotic diffusion and the origin of comets from the 2/3 resonance in the Kuiper belt. Icarus 127, 1–12.

Morbidelli, A., 1999. An overview on the Kuiper belt and on the origin of Jupiter-family comets. Celest. Mech. Dynam. Astron. 72, 129–156.

Stern, S.A., 1995. Collisional time scales in the Kuiper disk and their implications. Astron. J. 110, 856–868.

Stern, S.A., Colwell, J.E., 1997. Accretion in the Edgeworth–Kuiper belt: forming 100–1000 km radius bodies at 30 AU and beyond. Astron. J. 114, 841–849.

Trujillo, C.A., Jewitt, D.C., Luu, J.X., 2000. Population of the scattered Kuiper belt. Astrophys. J. 529, L103–L106.

Trujillo, C.A., Jewitt, D.C., Luu, J.X., 2001. Properties of the trans-neptunian belt: statistics from the Canada–France–Hawaii telescope survey. Astron. J. 122, 457–473.

Wisdom, J., Holman, M., 1991. Symplectic maps for the N-body problem. Astron. J. 102, 1528–1538.